UDC 620.192:681.78 https://doi.org/10.15407/vidbir2025.53.039

DETECTION AND IDENTIFICATION OF INTERNAL DEFECTS IN CFRP-CONCRETE BONDED JOINT USING OPTICAL-ACOUSTIC SYSTEM

L. I. Muravsky [1], M. Dutkiewicz [2], O. M. Sharabura [1], O. G. Kuts [1], O. V. Panchenko [3]

[1] Karpenko Physico-Mechanical Institute of the National Academy of Sciences of Ukraine, Lviv;

[2] Bydgoszcz University of Sciences and Technology, Bydgoszcz, Poland;

[3] Sika Ukraine, Kyiv

E-mail: muravskyleon@gmail.com

The optical-acoustic system (OAS) breadboard for detection and identification of internal defects implementing the developed optical-acoustic method is considered. The CFRP-concrete bonded joint sample containing the CFRP tape Sika CarboDur M514 and two elliptical debonding defects is prepared. The elliptical optical spatial responses from these defects at the OAS output are obtained at the fundamental resonance frequencies. The theoretical fundamental resonance frequencies of debonding defects are calculated using the formula for elliptical orthotropic plate and received orthotropic elastic constants of the CFRP tape. There is a slight deviation of the theoretical resonance frequencies from the experimental ones, which is explained by the small ratio of the sizes of defects to the depth of their occurrence. The subsurface portion of the crack in the test concrete beam was also detected using the OAS breadboard. Based on the developed OAS breadboard, it is possible to create simple and high-speed optical-digital systems for NDT of CFRP-concrete bonded joints used in civil and industrial engineering.

Keywords: *optical-acoustic system, CFRP-concrete bonded joint, optical-acoustic method, CFRP tape, elliptical debonding defect, dynamic speckle patterns, digital speckle pattern, optical spatial response, orthotropic elliptical plate, fundamental resonance frequency.*

ВИЯВЛЕННЯ ТА ІДЕНТИФІКАЦІЯ ВНУТРІШНІХ ДЕФЕКТІВ У КЛЕЙОВОМУ З'ЄДНАННІ "ВУГЛЕЦЕВА КОМПОЗИТНА СТРІЧКА–БЕТОН" ЗА ДОПОМОГОЮ ОПТИКО-АКУСТИЧНОЇ СИСТЕМИ

Л. І. Муравський [1], М. Дуткевич [2], О. М. Шарабура [1], О. Г. Куць [1], О. В. Панченко [3]

[1] Фізико-механічний інститут ім. Г. В. Карпенка Національної академії наук України, Львів;

[2] Бидгоська політехніка, Бидгощ, Польща;

[3] Сіка Україна, Київ

На основі розробленого оптико-акустичного методу створено макет оптико-акустичної системи (ОАС) для виявлення та ідентифікації еліптичних штучних міжфазних дефектів (непроклеїв) у клейовому з'єднанні "вуглецева композитна стрічка (ВКС)–бетон", а також тріщини, розташованої частково під поверхнею бетонної балки. Макет ОАС містить лазерну систему з амплітудною модуляцією, розширювач лазерного пучка, оптичну систему та цифрову камеру для реєстрації спекл-зображень, широкосмуговий генератор акустичних хвиль, п'єзоперетворювач, контролер та комп'ютер з відповідним програмним забезпеченням. Для виготовлення клейового з'єднання "ВКС–бетон" використали стрічку Sika CarboDur M514 та бетонну балку розмірами 160×40×40 мм, які з'єднували клеєм Sikadur 30. Непроклеї між ВКС та бетонною балкою формували за допомогою паперових шаблонів еліптичної і квадратної форми. Виготовлене клейове з'єднання вводили в макет ОАС і збуджували ВКС пружними згинальними хвилями в діапазоні від 1 до 100 кГц. Під час плавної зміни частоти збудження ВКС виявлено резонансні частоти ділянки її поверхні, розташованої безпосередньо над непроклеєм області інтересу (ОІ), яку розглядали як закріплену по краях мембрану з розмірами, які відповідали розмірам не-

проклею. Непроклеї виявляли та ідентифікували за оптичними просторовими відгуками від вібруючої ОІ, що формувались на виході макета ОАС в результаті накопичення серій динамічних спекл-зображень, їх реєстрації у вигляді цифрових спекл-зображень та подальшої обробки. Оскільки в окресленому місці розташування квадратного шаблону на поверхні бетонної балки сформувався непроклей еліптичної форми через заповнення клеєм чотирьох вузьких ділянок біля вершин виділеного шаблоном квадрата, то на виході макета ОАС отримали два оптичні еліпсоподібні відгуки від двох непроклеїв. Для перевірки достовірності експериментального визначення фундаментальних резонансних частот виявлених непроклеїв використали формулу для резонансної частоти еліптичної закріпленої ортотропної мембрани. Щоб обчислити теоретичні фундаментальні частоти для непроклеїв, визначали необхідні ортотропні пружні константи ВКС Sika CarboDur M514. В результаті отримали резонансні частоти, які незначно відхиляються від експериментальних. Такі відхилення зумовлені здебільшого малим співвідношенням розмірів непроклеїв до глибини їх залягання h = 1,4 мм. За допомогою макета ОАС також виявили підповерхневу частину тріщини у бетонній балці. Розроблений макет ОАС є базовим для створення простої та швидкісної оптико-цифрової систем неруйнівного контролю з'єднань "ВКС–бетон", які широко використовують у цивільному та промисловому будівництві.

Ключові слова: *оптико-акустична система, клейове з'єднання "вуглепластик–бетон", оптико-акустичний метод, вуглепластикова стрічка, еліптичний непроклей, динамічні спекл-зображення, цифрове спекл-зображення, оптичний просторовий відгук, ортотропна еліптична пластина, фундаментальна резонансна частота.*

Introduction. Recently, carbon fiber reinforced polymer (CFRP)-concrete bonded joints has been widely used in building industry. Strengthening of concrete, stone, metal, masonry and wooden structures using CFRP tapes results in increased shear and bending load-bearing capacity and enhanced ductility of structural reinforcement systems and joints in civil and industrial engineering. However, internal and, in paricular, interfacial defects between CFRP and concrete present in these structures, including debonding defects and cracks, can affect their durability and crack growth resistance. Therefore, non-destructive testing (NDT) of CFRP-concrete bonded joints is a relevant means of monitoring them during producing and operation.

There are several NDT techniques designed to detect internal defects in laminated composite structures and CFRP-concrete bonded joints. The most popular are Ultrasonics, Acoustic Emission Testing, Infrared Thermography, as well as Microwave, Optical Imaging, Ground Penetrating Radar, Radiography and Superconducting Techniques [1–3]. Among Optical Imaging Techniques, Electronic Speckle Pattern Interferometry and Digital Shearography occupy a leading position [4, 5]. The developed optical–acoustic method (OAM) due to its simplicity and operation speed [6–8] can be considered as an alternative to the above-mentioned interferometric techniques.

The objective of this study is to use the created optical-acoustic system (OAS) breadboard, designed on the basis of the developed OAM, to detect and identify elliptical debonding defects in an adhesive joint containing Sika CarboDur M514 tape and a test concrete beam bonded with Sicadur-30 glue, as well as to detect a crack located partially under the surface of the concrete beam.

Optical-acoustic method (OAM). The OAM is based on generating a series of dynamic speckle patterns (DNSPs) of the surface of a composite plate excited by elastic flexural waves. The DNSPs series after accumulation by a digital camera are used to produce the optical spatial responses from internal defects located below the composite surface [7, 8].

To apply the OAM for the CFRP-concrete bonded joint, an elastic wave with a smoothly increasing or decreasing frequency in both the ultrasonic (US) and sonic ranges is applied to the CFRP tape. At the same time, the surface area of the tape is illuminated by an expanded laser beam. The expanded laser beam is scattered on an optically rough surface of the tape, and an optical system containing a lens generates speckle patterns in the plane of the digital camera photodetector matrix. A series of

DNSPs formed in the plane of the photodetector matrix are recorded by a digital camera at equal time intervals with a duration τ, which is less than one fourth of the period T_{EW} of the flexural elastic wave oscillations. The digital camera records N pairs of digital speckle patterns (DSPs) with intensity distributions $I_{n1}(i, j)$ and $I_{n2}(i, j)$, where n=1,...,N is the number of the DSP pair I_{n1} and I_{n2}, (i, j) are the coordinates of pixels in the DSPs. Each n^{th} pair of DSPs I_{n1} and I_{n2} is recorded with the same exposure time t by accumulating P DNSPs for both DSPs I_{n1} and I_{n2} by a digital camera, with opposite polarities of the elastic wave amplitude A. To register the first DSP I_{n1} from the n^{th} pair, the DNSPs are accumulated at equal time intervals τ, the half-duration moments of which fall on the decline of the amplitudes of the elastic wave of one polarity. To register the second DSP I_{n2} from the n^{th} pair, the DNSPs are accumulated at the same time intervals τ, the half-duration moments of which fall on the decline of the amplitudes of the elastic wave of the opposite polarity. When a desired internal defect, in particular a debond, enters in the field of view of the digital camera, a section of the CFRP tape located directly above the defect, i.e. the region of interest (ROI), vibrates at its own fundamental or multiple resonance frequencies during excitation of the tape by flexural elastic waves. The ROI can be considered as a thin membrane with clamped edges coinciding with the edges of the internal defect [6–8], that is, the ROI dimensions correspond to the dimensions of the defect. The obtained DSPs are subtracted from each other and form the difference DSPs. This procedure can be repeated N times, and, summing all the difference DSPs pixel by pixel, the final difference DSP, or the flaw map, is formed [7, 8]. The resulting flaw map is analyzed for the presence of local zones of increased brightness, i.e. the optical spatial responses that display internal defects. The optical spatial response arises from the oscillating ROI, and its dimensions are commensurable with dimensions of the ROI and, accordingly, the internal defect. The size and area of the internal defect are determined by calculating the size and square of optical spatial responses. During a smooth and monotonous change in the frequency of flexural elastic waves in the field of view of the digital camera, optical spatial responses can appear in different places and at different frequencies. This indicates the presence of several defects on the composite tape surface area, which is in the field of view of the digital camera.

Optical-acoustic system. To implement the OAM, the OAS breadboard was developed. The block-diagram of the breadboard is shown in Fig. 1. The breadboard works as follows. The laser beam generated by the amplitude-modulated laser system *1* falls on the laser beam expander *2* to illuminate the surface area *3* of the CFRP tape *4*, bonded by a layer of glue *5* to the concrete beam *6*. If the surface area *3* is optically rough, then the light scattered on it, passing through the lens *7* of the digital camera *8*, forms DNSPs in the field of view of this camera. If the surface of the CFRP tape is optically smooth, the white paint or other light-colored paint is sprayed onto it to form DNSPs in the plane of the photodetector matrix.

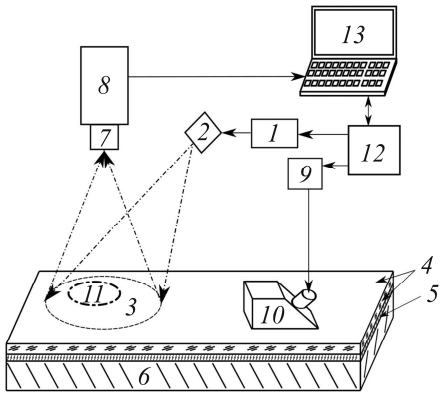

Fig. 1. Block-diagram of the optical-acoustic system breadboard: *1* – amplitude-modulated laser system; *2* – laser beam expander; *3* – surface area of CFRP tape; *4* – CFRP tape; *5* – layer of glue; *6* – test concrete beam; *7* – lens; *8* – digital camera; *9* – broadband acoustic wave generator; *10* – piezoelectric transducer; *11* – region of interest; *12* – control unit; *13* – computer.

The CFRP tape *4* is excited by a frequency chirping harmonic elastic wave using a broadband acoustic wave generator *9* and a piezoelectric transducer *10*. At one of the resonance frequencies, the ROI *11* above the interfacial defect begins to oscillate. Synchronously with the same moments of reaching the selected instantaneous amplitude value in the period T_{EW} of the elastic wave, the control unit *12* turns on the amplitude-modulated laser system *1* for equal time intervals τ and records the DSPs with the intensity distributions I_{n1} and I_{n2}, each of which is accumulated for the same number P ($P > 25$) of periods T_{EW} of the elastic wave at a given exposure of the digital camera *8*. The received DSPs are sent to computer *13* for further processing. The developed software calculates the sizes of the detected defects. The OAS breadboard is controlled using the control unit *12* and the computer *13*.

Detection and identification of artificial debonds. To study the possibility of detecting and identifying the artificial interfacial defects (debonds) in CFRP-concrete bonded joints, the joint sample containing two debonds was prepared. This sample was made by gluing a CFRP tape Sika CarboDur M514 with a concrete beam. The thickness of the CFRP tape is h=1.4 mm and its sizes are 160×40 mm, which coincide with the sizes of the surface of the concrete beam with sizes 160×40×40 mm. An elliptical template and a square template with a thickness of 0.4 mm (see Fig. 2*a*) were used to create artificial debonds No. 1 and No. 2, respectively, between the CFRP tape and the concrete specimen. Positions and dimensions of the templates in mm are indicated in Fig. 2*b*.

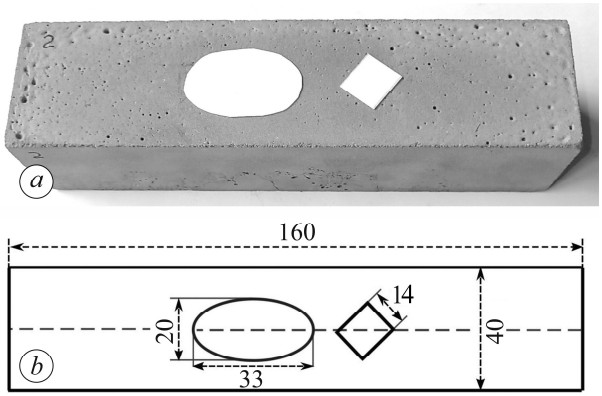

Fig. 2. Producing the artificial debonding defect (defects No. 1 on the left and defect No. 2 on the right) between the CFRP tape Sika CarboDur M 514 and test concrete beam; two templates on the concrete beam surface designed for making defects (*a*); sizes of the templates and beam in mm (*b*).

The CFRP tape was glued to the concrete beam using Sikadur-30 glue, and its surface was painted by a white aerosol spray-on paint to provide the developed speckles in generated DNSPs. In the outlined location of the square template on the concrete beam surface, an elliptical debond was formed due to filling with glue four narrow areas near the vertices of the square highlighted by the template. These areas have the shape of right triangles with a curved hypotenuse concave towards the right angle. We checked the ellipticity of the defect No. 2 by tapping the CFRP tape surface with various instruments. In the area of the defect, the frequency (tonality) of sounds from impacts on the tape surface changed. We also checked the effect of filling square defects with glue along the edges visually on a composite plate with square subsurface defects at a depth of 0.5 mm by illuminating the plate with an optical projector with a 100 W incandescent lamp. Then we tapped the surface over the defects to estimate their actual size without visual inspection. The results of estimating the size of square defects both the visual and tapping methods showed a high degree of agreement. So, as a result of

such filling of areas near the vertices of the square with glue, we obtained an elliptical debond No. 2. The produced CFRP-concrete bonded joint sample was inserted in the OAS breadboard and excited by elastic waves in a wide frequency range from 0.1 to 100 kHz. Lenses SP-L-C-16HKKS (focal length F = 16 mm) and "VEGA 2/20" (F = 20 mm) were used to record DNSPs of the studied surface area. With a smooth and monotonic increase in the elastic wave frequency, the optical spatial responses from the two artificial defects and from the edges of the sample appeared at their fundamental and multiple frequencies.

Fig. 3 shows flaw maps covering the field of view of 79.3×60 mm^2 received in the imaging optical system containing the lens SP-L-C-16HKKS. Fig. 3*a* shows the optical spatial response from the larger elliptical debonding (defect No. 1) at the fundamental resonance frequency $f_{01.1}$=14.5 kHz. The square template also produces the smaller elliptical debonding (defect No. 2), the optical spatial response from which at the fundamental resonance frequency $f_{01.2}$=40.7 kHz is shown in Fig. 3*b*. These responses have a ring-shaped form, which is explained by dominant influence of the ROI tilts on their creation. The optical responses at the frequency $f_{01.3}$=45.5 kHz indicate the presence of narrow and long debondings on the two opposite edges of the composite tape.

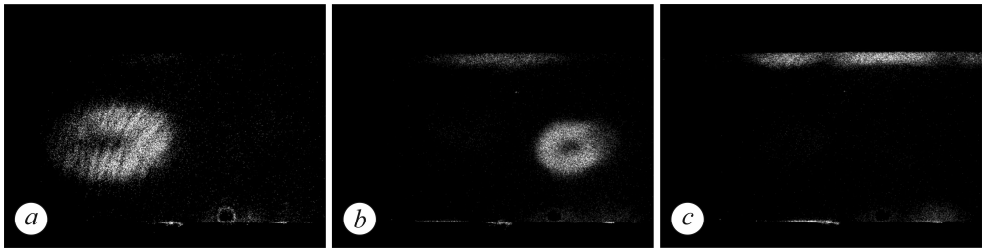

Fig. 3. Flaw maps of the studied areas (field of view 79.3×60 mm^2) of the CFRP-concrete bonded joint sample: optical spatial response from the defect No. 1 at the fundamental resonance frequency $f_{01.1}$=14.5 kHz (*a*); optical spatial response from the defect No. 2 at the fundamental resonance frequency $f_{01.2}$ = 40.7 kHz (*b*); optical spatial responses from narrow and long debondings on the two opposite edges of the composite tape at the frequency $f_{01.3}$ = 45.5 kHz (*c*).

Let us compare the experimental fundamental frequencies of the elliptical defects No. 1 and No. 2 with theoretical ones, which can be found from the known equation for the oscillating elliptical orthotropic plate, i.e. in our case the elliptical ROI with rectangular orthotropy, given by the formula [9]

$$\left(2\pi f_{01t}\right)^2 = \frac{41.52}{\rho h}\left(\frac{D_x}{a^4} + \frac{2}{3}\frac{D_{xy}}{a^2 b^2} + \frac{D_y}{b^4}\right). \qquad (1)$$

Here, ρ is the material density; h is the thickness of the CFRP tape and at the same time the depth of the debondings; a and b are the semimajor and semiminor axes of the ellipse; D_x, D_y are the flexural rigidities and D_{xy} is the torsional rigidity for principal directions of elasticity x and y of the CFRP tape. These rigidities are given by [10]

$$\left.\begin{aligned} D_x &= \frac{E_x h^3}{12\left(1-\nu_x\nu_y\right)} \\ D_y &= \frac{E_y h^3}{12\left(1-\nu_x\nu_y\right)} \\ D_{xy} &= D_x\nu_y + \frac{G_k h^3}{12} \end{aligned}\right\}, \qquad (2)$$

where E_x and E_y are the flexural moduli for the principal directions of elasticity, ν_x and ν_y are the Poisson's ratios, and G_k is the torsional shear modulus.

After substitution of Eq. (2) into Eq. (1), we receive the working equation for calculation of f_{01t}, that is

$$f_{01t} = \frac{3.72h}{2\pi\sqrt{\rho}}\sqrt{\frac{E_x}{4a^4(1-\nu_x\nu_y)} + \frac{\nu_y E_x}{6a^2b^2(1-\nu_x\nu_y)} + \frac{G_k}{3a^2b^2} + \frac{E_y}{4b^4(1-\nu_x\nu_y)}}. \quad (3)$$

This equation contains the known characteristics of the Sika CarboDur M1214 tape, namely, its thickness h = 1.4 mm, density ρ = 1600 kg/m^3 and Poisson ratio ν_x = 0.3. In [8] we have determined the flexural moduli of the Sika CarboDur M1214 tape according to the International Standard ASTM D790–17 [11]. Guided by this Standard, a series of test specimens of this material with a width of 12.7 mm were cut out, and, using the 3-point bending scheme, the flexural moduli were found to be E_x = 160 ± 2.5 GPa, E_y = 9.5 ± 0.3 GPa with a 90% confidence interval. Since the Young's moduli of the Sika CarboDur M1214 and Sika CarboDur M514 tapes are equal, we use the obtained values of flexural moduli of the Sika CarboDur M1214 to calculate the frequency f_{01t} of the elliptical ROI located in the Sika CarboDur M514 tape, i.e., the elliptical artificial debonding defect No. 1 of width $2a_1$ = 33 mm and height $2b_1$ = 20 mm, shown in Fig. 2. The Poisson's ratio ν_y for the principal direction y can be found using the well-known dependence $\nu_x/E_x = \nu_y/E_y$, based on which we obtain ν_y=0.0178. As shown by Mottram [12], the individual layers of unidirectional pultruded fiber reinforced plastic material have torsional shear moduli, ranging from 3.5 to 4.8 GPa. Substituting the above values into Eq. (3), we receive the fundamental frequencies of an elliptical orthotropic plate of width $2a_1$ = 33 mm and height $2b_1$ = 20 mm, i.e. the ROI located above the defect No. 1, equal to $f_{01t.1}$=19.0 ÷ 19.2 kHz. As we can see, the frequencies differ from the experimentally obtained resonance frequency $f_{01.1}$=14.5 kHz of the defect No. 1. The width of the elliptical optical spatial response from this defect is $2a_{1e}$= 31.4 mm, and the height is $2b_{1e}$ = 19 mm, which is by 5% smaller than the width and height of the elliptical template shown in Fig. 2.

The width of the elliptical optical spatial response from the elliptical debonding defect No. 2 is $2a_{2e}$ = 18.52 mm, and the height is $2b_{2e}$ = 16.14 mm. If to assume that the dimensions of the defect No. 1 are equal to dimensions of the elliptical template (see Fig. 2), the real width of the defect No. 2 is $2a_2$ = 19.5 mm and the real height is $2b_2$= 17 mm. Substituting these dimensions and mentioned above values of orthotropic elastic constants and physical quantities of the Sika CarboDur M514 tape in Eq. (3), we obtain the theoretical fundamental resonance frequencies $f_{01t.2}$ = 46.9÷47.3 kHz for this defect, while its experimental fundamental resonance frequency is $f_{01.2}$ = 40.7 kHz.

Deviations of theoretical resonance frequencies from experimental ones can be explained by several factors, but the main factor is the small ratio of the debonding size to its depth of occurrence [13–15], which for the minor axis of the defect No. 1 is about 7:1, and for the minor axis of the defect No. 2 is about 6:1, which leads to a shift in the theoretical fundamental resonance frequencies toward higher values. Such tendency of the frequency shift is confirmed by similar experimental results obtained, in particular, by Crosbie et al. [15], Cawley and Theodorakopulos [16], and Solodov et al. [17].

Detection of a crack located partly beneath the surface of a test concrete beam. Among the test concrete beam specimens used to produce CFRP-concrete bonded joints, we found a specimen containing a crack located partly on the surface of a concrete beam and partly beneath its surface. To estimate the ability of the OAM to detect subsurface cracks in concrete beams, we placed this specimen in the OAS breadboard and excited it with elastic waves in the frequency range from 1 to 50 kHz. The imaging optical system in the OAS breadboard contained the lens "VEGA 2/20". The concrete beam

shown in Fig. 4 contains a crack located partly on the beam surface and partly beneath its surface. At a frequency of 2.1 kHz, a spatial response from the crack was recorded (see Fig. 5*a*), including its part located beneath the surface at the bottom of the beam shown in Fig. 4. At a frequency of 43.6 kHz, the crack initiation zone was detected, shown in Fig. 5*b*. It can be seen from Fig. 5*b* that the dimensions of the detected initiation zone exceed its dimensions observed during visual inspection of this beam.

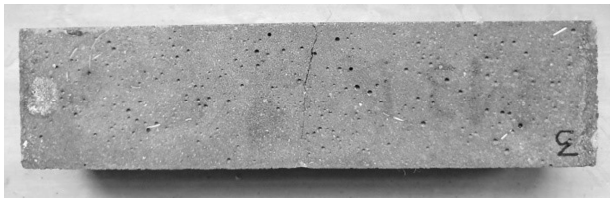

Fig. 4. Concrete beam.

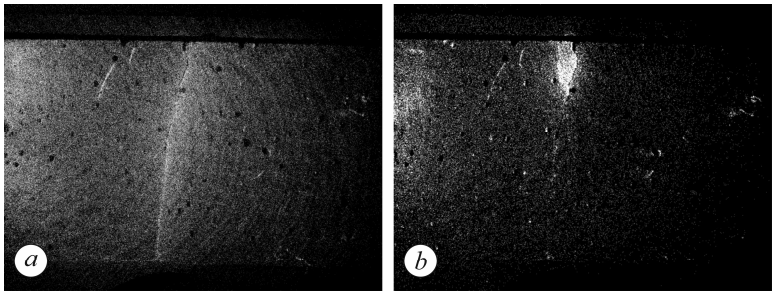

Fig. 5. Spatial responses from the crack at frequencies f = 2.1 kHz (*a*) and f = 43.6 kHz (*b*). The crack is partly located under the surface of the concrete beam.

CONCLUSION

The OAS breadboard implementing the OAM can detect and identify debonding defects in CFRP-concrete bonded joints at the depth h = 1.4 mm. Due to the excitation of CFRP tapes with elastic waves in the US and sonic ranges and the recording of a series of DNSPs, internal defects are detected at a high speed while simultaneously covering a large area of the CFRP tape surface. The deviations of the theoretical fundamental resonance frequencies of artificial elliptical debonding defects, calculated using the working equation obtained for orthotropic elliptical plates, from the corresponding experimental resonance frequencies are relatively small and are caused mainly by small ratios of the sizes of defects to the depth of their occurrence. The developed OAS breadboard can be considered as the first step toward creation of simple and high-speed optical-digital systems for NDT of CFRP-concrete bonded joints used in civil and industrial engineering.

1. Halabe, U.B. Non-destructive evaluation (NDE) of composites: techniques for civil structures. *Nondestructive evaluation (NDE) of polymer matrix composites*; Karbhari, V.M., Ed.; Woodhead Publishing Limited, 2013; pp 483–514. https://doi.org/10.1533/9780857093554.4.483
2. Rasheed, H.A. *Strengthening Design of Reinforced Concrete with FRP*; Taylor & Francis Group, LLC, 2015. https://doi.org/10.1201/b17968
3. Dolati, S.S.K.; Malla, P.; Ortiz, J.D.; Mehrabi, A.; Nanni, A. Identifying NDT methods for damage detection in concrete elements reinforced or strengthened with FRP. *Eng. Struct.* **2023**, *287*, 116155. https://doi.org/10.1016/j.engstruct.2023.116155
4. Taillade, F.; Quiertant, M.; Benzarti, K.; Aubagnac, C.; Moser E. Non-destructive evaluation (NDE) of composites: Using shearography to detect bond defects. *Nondestructive evaluation (NDE) of polymer matrix composites*; Karbhari, V.M., Ed.; Woodhead Publishing Limited, 2013; pp 542–557. https://doi.org/10.1533/9780857093554.4.542

5. Zhang, X.; Wang, H.; Peng, H.; Du, H.; Jiao, Y.; Li, S.; Zhang, J.; Pan, Z.; Huang, H.; Ju, Y. A DSSPI phase unwrapping method for improving the detection efficiency of CFRP-reinforced concrete defect. *Opt. Laser Technol.* **2024**, *168*, 109862. https://doi.org/10.1016/j.optlastec.2023.109862
6. Nazarchuk, Z.T.; Muravsky, L.I.; Kuts, O.G. Nondestructive testing of thin composite structures for subsurface defects detection using dynamic laser speckles. *Res. Nondest. Eval.* **2022**, *33*, 59–77. https://doi.org/10.1080/09349847.2022.2049407
7. Nazarchuk, Z.; Muravsky, L.; Kuryliak, D. Methods for processing and analyzing the speckle patterns of materials surfaces. *Optical metrology and optoacoustics in nondestructive evaluation of materials;* Nazarchuk, Z., Muravsky, L., Kuryliak, D., Eds.; Springer Nature, 2023; pp 249–323. https://doi.org/10.1007/978-981-99-1226-1_6
8. Muravsky, L.; Nazarchuk, Z.; Kuts, O.; Ivanytskyi, Ya.; Sharabura, O. Detecting of interfacial defects in CFRP–concrete bonded joints using dynamic speckle patterns of excited surface. *NDT&E* **2025**, *156*, 103480. https://doi.org/10.1016/j.ndteint.2025.103480
9. Leissa, A.W. *Vibration of Plates*; National Aeronautics and Space Administration: Washington, DC, 1969.
10. Lekhnitskii, S.G. *Anisotropic Plates;* Gordon and Breach Science Publishers, 1968.
11. ASTM International. *Standard Test Methods for Flexural Properties of Unreinforced and Reinforced Plastics and Electrical Insulating Materials*, ASTM D790-17; West Conshohocken, PA, 2017.
12. Mottram, J.T. Shear modulus of standard pultruded fiber reinforced plastic material. *J. Compos. Constr.* **2004**, *8*, 141–147. https://doi.org/10.1061/(ASCE)1090-0268(2004)8:2(141)
13. Srinivas, S.; Joga Rao, C.V.; Rao, A.K. An exact analysis for vibration of simply supported homogeneous and laminated thick rectangular plates. *J. Sound Vib.* **1970**, *12* (2), 187–199. https://doi.org/10.1016/0022-460X(70)90089-1
14. Eratlı, N.; Aköz, A.Y. The mixed finite element formulation for the thick plates on elastic foundations. *Comput. Struct.* **1997**, *65* (4), 515–529. https://doi.org/10.1016/S0045-7949(96)00403-8
15. Crosbie, R.A.; Dewhurst, R.J.; Palmer, S.B. Flexural resonance measurements of clamped and partially clamped disks excited by nanosecond laser pulses. *J. Appl. Phys.* **1986**, *59* (6), 1843–1848. https://doi.org/10.1063/1.336410
16. Cawley, P.; Theodorakopoulos, C. The membrane resonance method of non-destructive testing. *J. Sound. Vib.* **1989**, *130* (2), 299–311. https://doi.org/10.1016/0022-460X(89)90555-5
17. Solodov, I.; Rahammer, M.; Kreutzbruck, M. Analytical evaluation of resonance frequencies for planar defects: Effect of a defect shape. *NDT&E* **2019**, *102*, 274–280. https://doi.org/10.1016/j.ndteint.2018.12.008

Received 20.03.2025

ORCID iDs

Muravsky L.I. https://orcid.org/0000-0001-8839-2819
Dutkiewicz M. https://orcid.org/0000-0001-7514-1834
Sharabura O.M. https://orcid.org/0000-0002-5712-4114
Kuts O.H. https://orcid.org/0000-0003-1659-9452
Panchenko O.B. https://orcid.org/0000-0003-1634-0715